Article ID: 1000-324X(2015)09-1002-07 **DOI:** 10.15541/jim20150124

Facile Synthesis of Visible Light Activated Carbon-incorporated Mn Doped TiO_2 Microspheres *via* Flame Thermal Method

SUN Tong, CHEN Yang, MA Xiao-Qing, LI Zhong, LI Hui, CUI Xiao-Li

(Department of Materials Sciences, Fudan University, Shanghai 200433, China)

Abstract: Carbon-incorporated Mn doped TiO_2 (C/Mn-TiO_2) microspheres with different Mn contents were prepared by a facile and novel flame assisted approach. The influence of the Mn contents on the morphology and performance was investigated by X-ray diffraction (XRD), field emission scanning electron microscopy (FE-SEM), ultraviolet-visible diffuse reflectance spectroscopy (DRS), X-ray photoelectron spectra (XPS) and Raman spectra, respectively. SEM and XRD results showed the existence of anatase TiO_2 microspheres without post-heat treatment. XPS and Raman results confirmed Mn^{2+} substitution of Ti^{4+} in the resulted samples. UV-Vis diffuse reflectance spectra showed that the incorporation of Mn into TiO_2 lattice could enhance visible light absorption. Improved photocatalytic activity for the degradation of methylene blue (MB) under visible light illumination was demonstrated with the introduction of Mn dopant. The introduction of Mn resulted in the narrowed band gap in C/Mn-TiO_2. This study offers not only an environmentally friendly product with high photocatalytic activity, but also a rapid and direct strategy without any particular skill.

Key words: TiO_2; photocatalyst; flame thermal method; microsphere; Mn doped

TiO_2 has been widely exploited for various applications, such as purification of air, bactericidal action, self-cleaning, and degradation of organic pollutant compounds in wastewater[1-2]. However, TiO_2 is known as a wide band gap semiconductor (3.0 eV for rutile and 3.2 eV for anatase)[3]. This means TiO_2 can only be activated by UV irradiation. Besides, the fast recombination of photoinduced electrons and holes leads to a lower efficiency of photoquantum. Therefore, it is of great importance to develop efficient visible light responsive photocatalysts by modification of TiO_2[4].

The doping of transition metals has been widely studied in order to improve the photocatalytic performance of TiO_2, such as doping with Fe[5-6], Cr[7], V[8], Mn[9-12], *etc*. Deng, *et al*[10] prepared Mn-doped TiO_2 powders by Sol-Gel method, and followed by further calcination. Their results showed that the introduction of Mn dopants could improve the photocatalytic activity of TiO_2 and the optimum amount of Mn dopants was 0.2at%. Liu, *et al*[11] fabricated Mn-doped TiO_2 by reactive magnetron sputtering deposition at 550℃. The incorporation of Mn in the TiO_2 lattice introduced intermediate band into its narrowed forbidden gap, leading to remarkable red-shifts in the optical absorption edges. However, their synthesized methods relied highly on expensive equipment or complicated experiment process, which may hinder its wide applications. It is still a great challenge to search for effective and facile approaches to prepare Mn doped TiO_2 photocatalysts.

Recently, we have developed an easy and facile method to synthesize carbon-incorporated titanium dioxide (C/TiO_2)[13-14], Ta_2O_5[15] and Nb_2O_5[16] powders with the advantage of simple processing, short reaction time and only one step to final product with improved photocatalytic activities. This new approach provides the feasibility for the preparation of other modified TiO_2 materials with higher photocatalytic performance. We are highly interested in whether this method is suitable for the fabrication of Mn-doped TiO_2 and its photocatalytic activity. Herein, we synthesized Mn doped C/TiO_2 materials and demonstrated their enhanced photocatalytic activity in this work. Influences of Mn content on the phase composition, morphology, and photocatalytic performance of the samples were discussed, respectively.

1 Experimental

1.1 Preparation of C/Mn-TiO_2 photocatalysts

Tetrabutyl orthotitanate (98%, TBOT), absolute ethanol

Received date: 2015-03-12; **Modified date:** 2015-04-26; **Published online:** 2015-06-02
Foundation item: National Natural Science Foundation of China (21273047); National Basic Research Program of China (2011CB933300)
Biography: SUN Tong(1990–), male, candidate of master degree. E-mail:12210300031@fudan.edu.cn
Corresponding author: CUI Xiao-Li, professor. E-mail: xiaolicui@fudan.edu.cn

(AR) and manganese (II) acetyllacetonate were used as received to prepare C/Mn-TiO_2 materials. By controlling different amounts of manganese (II) acetyllacetonate with molar ratio of Mn to Ti varying from 0.1mol% to 1mol%, the ternary mixtures of 35 mL ethanol, 5 mL of TBOT and the required amount of manganese (II) acetyllacetonate were homogeneously mixed. Then the mixed stable and clear solution were ignited by a burning match, respectively. The combustion process was gentle and gray powders can be obtained finally. The as-prepared samples were denoted as C/X-Mn-TiO_2(X represents the molar content of Mn). For comparison, C/TiO_2 was also prepared by the same method with the absence of manganese (II) acetyllacetonate.

1.2 Characterizations

The phase composition of the resulted samples were characterized by XRD on a Bruker D/8 advanced diffractometer using Cu Kα and laser Raman microspectroscopy (He-Cd UV laser, excitation source of wavelength 442 nm, Renishaw in Via). The X-ray photoelectron spectroscopy (XPS) was measured using a RBD upgrated PHI-5000C ESCA system (Perkin Elmer) with Mg Kα radiation with the binding energies calibrated based on the contaminant (C1s-284.6 eV). The morphologies and microstructures were characterized using FE-SEM (Philips XL30). EDAX Genesis system was applied for the elemental analysis. The UV-vis diffuse reflectance spectra (DRS) were recorded using a Cary-500 Scan UV-vis spectrophotometer.

1.3 Photocatalytic experiments

The photocatalytic reactor is made of quartz tube with inner diameter of 6 mm and length of 304.8 mm. The cooling jacket around the reactor can effectively preclude IR part of the spectra from penetrating into the reactor. This design helps in cooling the lamps along to maintain constant reactor temperature. A specific amount (25 mg) of each photocatalyst powder was suspended in 10 mL of methyl blue (MB, 5 mg/L) aqueous solution and kept in dark for 2 h to achieve adsorption/desorption equilibrium. The of the suspension temperature was maintained at 25.0℃ during the photocatalytic reaction and 3 mL of MB solution was taken out every 20 min to analyze the concentration of MB with UV-Vis absorption spectroscopy.

2 Results and discussion

Figure 1 shows XRD patterns of C/TiO_2 and C/Mn-TiO_2 with varying dopant levels. As seen in Fig. 1, these peak positions revealed that all of the samples consisted only of anatase and secondary phases resulting from the doping of Mn were not present or below the level of detection of the instrument. The absence of Mn suggests that Mn may be incorporated in TiO_2 lattice or their respective oxides are present at levels below detection level of XRD, which agrees with the previous reports[10, 17-21]. The (101) peak gradually shifts with the introduction of Mn as shown in inset of Fig.1, an enlarged view of the XRD patterns. The shift of the (101) peak can be attributed to the substitution of large sized Mn^{2+}(0.080 nm) on the Ti^{4+}(0.068 nm) site of anatase TiO_2[22].

Chemical analysis has been performed with X-ray photoelectron spectroscopy as shown in Fig. 2. Figure 2(a) shows the finely scanned Ti2p peak of the samples. Two peaks with binding energies of 458.6 eV and 464.3 eV were observed, which could be attributed to Ti2p3/2 and Ti2p1/2 for Ti (IV) of titania, respectively[23-24]. Additionally, the position of the Ti2p peaks showed slight shifts toward higher energies compared to the values of the bare TiO_2, the shift of peaks can support the doping of Mn ions into the TiO_2 lattice[7, 25]. Figure 2(b) and Fig. 2(c) showed the XPS of C1s core level of the samples. Three peaks at 284.6, 285.7 and 288.6 eV can be identified, respectively. The strong peak at 284.6 eV was assigned to elemental carbon, arising from the incomplete burning of organic compounds, and the adventitious carbon absorbed on the surface of the sample. The other two small peaks were assigned to C–O bonds, which can be attributed to the insufficient hydrolysis of TBOT.

Figure 2(d) and Fig. 2(e) showed the XPS spectra of O1s core level of the samples. Only two peaks occured at 531.5 and 530.1 eV for C/TiO_2 in Fig. 2(d), which could be attributed to –OH on the surface and Ti–O–Ti. Four peaks at 532.8, 531.4, 530.8 and 529.9 eV can be identified for C/0.5%Mn–TiO_2 as shown in Fig. 2(e), which were assigned to C–O, –OH on the surface, Ti–O–Ti and Ti–O– Mn, respectively[13, 26].

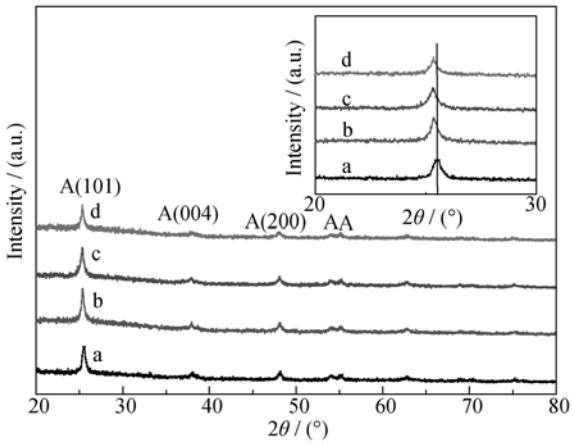

Fig. 1　XRD patterns of the as-prepared C/TiO_2 (a) and C/Mn-TiO_2 (b-d)

The content of Mn in samples (b-d) is 0.1% (b), 0.5% (c) and 1% (d), respectively. (A: anatase) and the enlarged view of the (101) peak position (insert)

However, the actual valences of Mn could not be determined owing to their low concentrations[9, 19, 27]. Laser Raman microspectroscopy is a better choice in the detection of very low levels of secondary phases considering the much higher sensitivity. The Raman spectra of C/TiO_2 and C/0.5%Mn-TiO_2 are shown in Fig. 2(f). All of the fabricated samples were composed of anatase (peaks at ~144 and 639 cm^{-1}), which agrees well with the XRD results. While, the shift of Raman peak at ~144 cm^{-1} for Mn-doped samples was observed compared to the undoped sample. Since the laser Raman spectra signal depends on vibrational models, the formation of the solid solution caused the alteration of the lattice and the associated peak shift. The lowest-frequency E_g mode is closely related to the grain size of the TiO_2 nanoparticles. This mode is sensitive to local oxygen coordination surrounding the metal ion[28].

The expanded view of this mode in the inset of Fig. 2(f) shows that the Raman E_g peak. The peak of TiO_2 becomes blue shifted as TiO_2 is incorporated with Mn. The radius of Mn^{2+} is 0.080 nm, which is higher than that of Ti^{4+} (0.068 nm)[27]. If doping occurs at a substitutional position on the Ti^{4+} site, the Ti–O–Ti bond would partly be removed due to the formation of a Mn–O–Ti bond. The strength of a bond is determined by its force constant which is associated with frequency by $v \propto k^{1/2}$[29]. Therefore, the decreasing ratio of Ti–O/Mn–O bonds will contract the lattice, thus shifting the E_g position to higher wave number. Hence the formation of new Ti–O–Mn bonds and the removal of the Ti–O–Ti bond can be explained from the shifting of Raman peak[19]. This confirms the Mn^{2+} substitution of Ti^{4+}[18, 21].

Figure 3 shows the SEM images for the morphology of the resulted samples. As seen in Fig. 3, TiO_2 spheres are 1–3 μm in diameter. No obvious differences are observed with Mn dopant concentration below 1%. The EDX is carried out on the selected area of the sample as shown in Fig. 4. The EDX spectra of the sample confirmed the presence of Ti, O, C and Mn.

The absorption spectra show the optical properties of the synthesized samples (Fig. 5). The band structure of pristine semiconductor TiO_2 is made up of Ti3d level and O2p level which forms conduction band and valence band, respectively, corresponding to the fundamental absorption edge at 380 nm[27]. The introduction of Mn dopants caused the shifting of the absorption edge of TiO_2.

TiO_2 exhibits both direct and indirect band gap. However, a lot of work shows that indirect band gap is more common in anatase TiO_2[30]. The band gap values of each samples are shown in Table 1 and Fig. 6, respectively. The effective optical band gap of TiO_2 is reduced to 3.19, 3.00, 2.87 and 2.73 eV as incorporation of 0, 0.1%, 0.5%, 1% Mn, respectively.

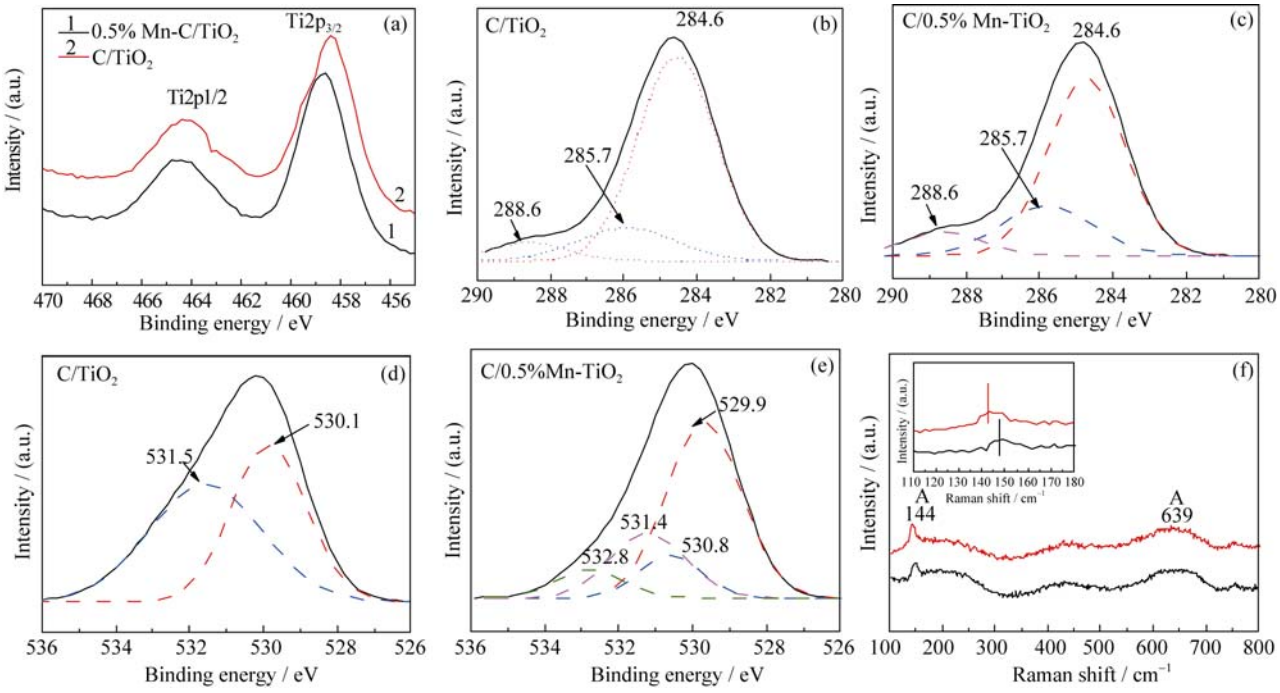

Fig. 2 XPS spectra (a-e) and laser Raman spectra (f) for the samples

XPS for Ti2p core level (a), C1s core level of C/TiO_2 (b) and C/0.5% Mn-TiO_2 (c), O1s core level of C/TiO_2 (d) and C/0.5% Mn-TiO_2 (e). Laser Raman spectra (f) of C/TiO_2 (red), C/0.5% Mn-TiO_2 (black), respectively, and the enlarged view of the intense E_g peak (insert in (f))

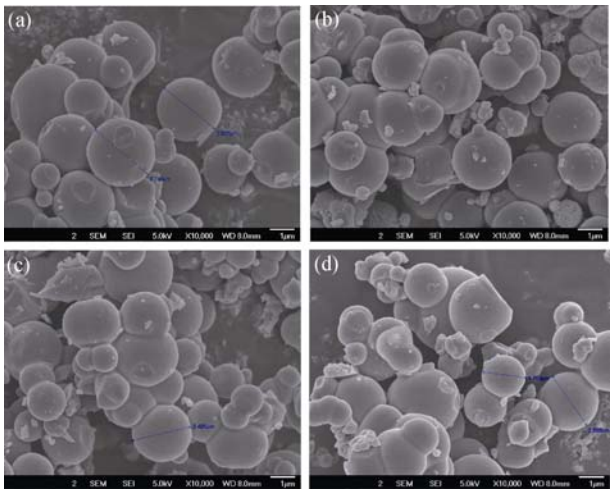

Fig. 3　SEM images of the as-prepared C/TiO_2 (a) and C/Mn-TiO_2 (b-d)

The content of Mn in samples is 0.1% (b), 0.5 % (c) and 1% (d), respectively

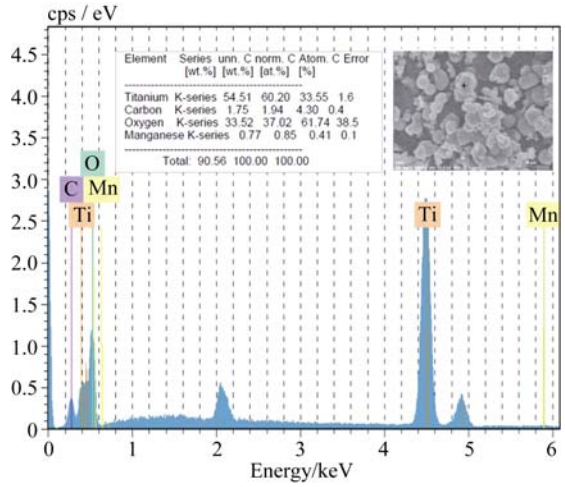

Fig. 4　EDX spectra of C/1% Mn-TiO_2

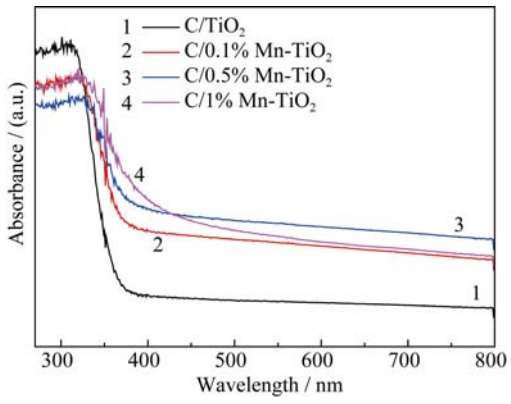

Fig. 5　UV-Vis diffuse reflectance spectra of as-prepared C/TiO_2 and C/Mn-TiO_2

This reduction can be attributed to band gap renormalization effect. In consistency with this effect, introduction of extra electrons in the form of Mn leads to the hybridization of the d-states of Mn with the conduction band edge of the host. This effect leads to an uplift of the valence band maximum and downward shift of the conduction band minimum with an effective reduction in band gap[31]. The interaction of the electrons in d-states of Mn with the host conduction electron is enhanced with the increase in the concentration of the dopants, resulting in the lowering of the effective band gap of TiO_2[22]. Shao, *et al* calculated the band gap of Mn-doped TiO_2 *via* DFT method and explained that the introduction of Mn dopant could create Mn d-states in the band gap and interaction of these d-states with the host electrons, thus leading to narrowed band gap[32].

The photocatalytic activities of the as-prepared materials were carried out under visible light irradiation. MB was used as the model contaminant, a dye widely used as an indicator to study the photocatalytic activities of different photocatalysts[33] . MB exhibits absorption peaks in the visible light. Thus, monitoring the absorbance at 664 nm is a good method to analyze the degradation content *via* optical absorption spectroscopy. We studied the photodegradation of MB in C-TiO_2 and subsequently in C/Mn-TiO_2 in different contents by irradiating a mixture of photocatalyst and MB with visible light.

Figure 7 shows the linear relationship between $\ln(C_0/C)$ and reaction time for different TiO_2 photocatalysts prepared in this work. All these plots were matched to the first-order reaction kinetics, and the reaction rate constant (k) can be calculated from the rate equation of $\ln(C_0/C)=kt$ (inset in Fig. 7), which can be used as an indication of the photocatalytic activity. All the C/Mn-TiO_2 exhibited improvement in photocatalytic activity compared to the bare C/TiO_2. It was found that the photocatalytic activity increased first and then decreased with increasing Mn dopants concentration. Especially,the optimal

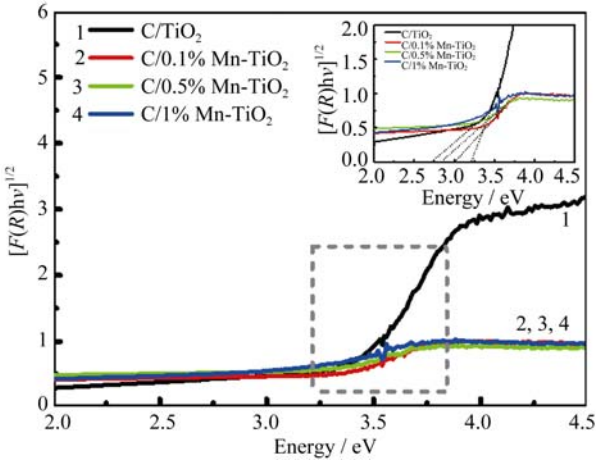

Fig. 6　Band gaps of as-prepared C/TiO_2 and C/Mn-TiO_2

Table 1　Optical indirect band gaps of C/TiO_2 and C/Mn-TiO_2

Mn doping	0	0.1%	0.5%	1.0%
Optical indirect band gap /eV	3.19	3.00	2.87	2.73

photocatalytic activity was observed for C/0.5%Mn-TiO_2 among all the synthesized samples.

These results indicate that Mn-doped C/TiO_2 can lead to better photocatalytic activity compared to C/TiO_2. Carbon incorporated in TiO_2 microspheres could facilitate the charge transferring process and work as a kind of photo sensitizer of TiO_2[6, 13-14]. The introduction of Mn ions will induce an intermediate band into the forbidden gap of rutile TiO_2, splitting the forbidden gap into pseudo-direct upper and lower sub-gaps, which could narrow the band gap of TiO_2[11].The narrowed band gap enhanced the absorption of visible light and more charge carriers are generated[11, 32].The Mn^{2+} half-filled electronic structure can also accelerate charge transfer processes as the shallow trap for the charge carriers, which will enhance the photocatalytic activity of TiO_2. When Mn^{2+} (d^5) traps electron, electronic configuration changes to d^6 and if it traps holes its electronic configuration will be a highly unstable d^4 state[27]. The trapped electrons and holes will be transferred to generate superoxide radicals and hydroxyl radicals as shown in Eqs. (1) - (4)[34].

$$Mn^{2+}+e^- \rightarrow Mn^+ \quad (1)$$

$$Mn^++O_{2ads} \rightarrow Mn^{2+} + O_2^- \quad (2)$$

$$Mn^{2+}+h^+ \rightarrow Mn^{3+} \quad (3)$$

$$Mn^{3+}+OH^- \rightarrow Mn^{2+}+OH^{\cdot} \quad (4)$$

However, *k* value decreased when the Mn content increased to 1% in the sample, showing the poor photocatalytic performance. This may be attributed to the accelerated recombination process, thus significantly restricting the photocatalytic activity[35] .

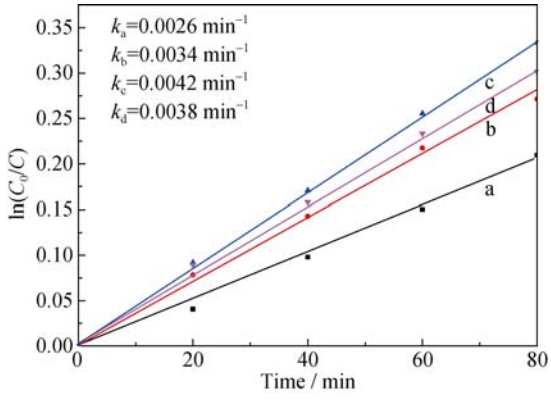

Fig. 7 Photocatalytic activity of the samples in degradation of MB under visible light illumination

C/TiO_2 (a) and C/Mn-TiO_2 (b-d). The content of Mn is 0.1% (b), 0.5% (c) and 1% (d), respectively

3 Conclusions

A facile approach towards the synthesis of carbon-incorporated Mn doped TiO_2 photocatalysts was developed by a one-step flame thermal method. XRD patterns showed that the crystal structure of all as-prepared samples was anatase TiO_2. The absorption edges of the materials were estimated from the absorption spectra and were demonstrated to shift to longer wavelength with the introduction of Mn dopants. The photocatalytic activity for degradation of MB was improved by the introduction of suitable amount of Mn, compared with that of C/TiO_2. The enhanced photocatalytic performance is attributed to its enhanced visible light absorption and unique half-filled electronic configuration. Furthermore, other codoped metal oxides based on their corresponding metal precursors could also be synthesized based on this simple and facile method.

References:

[1] CHEN P, HU Y, WEI C. Preparation of superhydrophilic mesoporous SiO_2 thin films. *Applied Surface Science*, 2012, **258(10):** 4334–4338.

[2] WANG J, WANG J, SUN Y, *et al*. The preparation of superhydrophilic surface of TiO_2 coating without ultraviolet irradiation through annealing treatment. *Journal of Sol-Gel Science and Technology*, 2013, **68(1):** 75–80.

[3] FUYUKI T, MASUNAMIM H. Electronic-properties of the interface between Si and TiO_2 deposited at very low-temperatures. *Japanese Journal of Applied Physics Part 1-Regular Papers Short Notes & Review Papers*, 1986, **25(9):** 1288–1291.

[4] UMEBAYASHI T, YAMAKI T, ITOH H, *et al*. Band gap narrowing of titanium dioxide by sulfur doping. *Applied Physics Letters*, 2002, **81(3):** 454–456.

[5] ZHU J F, ZHENG W, BEN H E, *et al*. Characterization of Fe-TiO_2 photocatalysts synthesized by hydrothermal method and their photocatalytic reactivity for photodegradation of XRG dye diluted in water. *Journal of Molecular Catalysis A-Chemical*, 2004, **216(1):** 35–43.

[6] CHEN X, LI H, SUN T, *et al*. One-step flame-assisted pyrolysis synthesis of Fe doped carbon incorporated TiO_2 and its photocatalytic activity. *Chemical Journal of Chinese Universities-Chinese*, 2013, **34(12):** 2855–2860.

[7] ZHU J F, DENG Z G, CHEN F, *et al*. Hydrothermal doping method for preparation of Cr^{3+}-TiO_2 photocatalysts with concentration gradient distribution of Cr^{3+}. *Applied Catalysis B-Environmental*, 2006, **62(3/4):** 329–335.

[8] KLOSEK S, RAFTERY D. Visible light driven V-doped TiO_2 photocatalyst and its photooxidation of ethanol. *Journal of Physical Chemistry B*, 2001, **105(14):** 2815–2819.

[9] BINAS V D, SAMBANI K, MAGGOS T, *et al*. Synthesis and

photocatalytic activity of Mn-doped TiO_2 nanostructured powders under UV and visible light. *Applied Catalysis B-Environmental*, 2012, **113(SI):** 79–86.

[10] DENG Q R, XIA X H, GUO M L, *et al*. Mn-doped TiO_2 nanopowders with remarkable visible light photocatalytic activity. *Materials Letters*, 2011, **65(13):** 2051–2054.

[11] LIU L, XIA X, LUO J K, *et al*. Mn-doped TiO_2 thin films with significantly improved optical and electrical properties. *Journal of Physics D-Applied Physics*, 2012, **45(48):** 485102.

[12] XIN W, ZHU D, LIU G, *et al*. Synthesis and characterization of Mn-C-Codoped TiO_2 nanoparticles and photocatalytic degradation of methyl orange dye under sunlight irradiation. *International Journal of Photoenergy*, 2012, **2012:** 767905–1–7.

[13] ZHANG X, SUN Y, CUI X, *et al*. Carbon-incorporated TiO_2 microspheres: facile flame assisted hydrolysis of tetrabutyl orthotitanate and photocatalytic hydrogen production. *International Journal of Hydrogen Energy*, 2012, **37(2):** 1356–1365.

[14] LI H, ZHANG X, CUI X. A facile and waste-free strategy to fabricate Pt-C/TiO_2 microspheres: Enhanced photocatalytic performance for hydrogen evolution. *International Journal of Photoenergy*, 2014, **2014:** 414281–1–9.

[15] LI J, CHEN X, SUN M, *et al*. A facile flame assisted approach to fabricate Ta_2O_5 microspheres. *Materials Letters*, 2013, **110:** 245–248.

[16] MA X, CHEN Y, LI H, *et al*. Annealing-free synthesis of carbonaceous Nb_2O_5 microspheres by flame thermal method and enhanced photocatalytic activity for hydrogen evolution. *Materials Research Bulletin*, 2015, **66:** 51–58.

[17] PUTLURU S S R, SCHILL L, JENSEN A D, *et al*. Mn/TiO_2 and Mn-Fe/TiO_2 catalysts synthesized by deposition precipitation- promising for selective catalytic reduction of NO with NH_3 at low temperatures. *Applied Catalysis B-Environmental.* 2015, **165:** 628–635.

[18] CHOUDHURY B, CHOUNDHURY A. Oxygen vacancy and dopant concentration dependent magnetic properties of Mn doped TiO_2 nanoparticle. *Current Applied Physics*, 2013, **13(6):** 1025–1031.

[19] QUAN F, HU Y, ZHANG X, *et al*. Simple preparation of Mn-N-codoped TiO_2 photocatalyst and the enhanced photocatalytic activity under visible light irradiation. *Applied Surface Science*, 2014, **320:** 120–127.

[20] LI X Y, WU S X, XU L M, *et al*. Effects of depositing rate on structure and magnetic properties of Mn: TiO_2 films grown by plasma-assisted molecular beam epitaxy. *Material Science and Enigineering B-Advanced Functional Solid-State Materials*, 2009, **156(1/2/3):** 90–93.

[21] LIN M Z, CHEN H, CHEN W F, *et al*. Effect of single-cation doping and codoping with Mn and Fe on the photocatalytic performance of TiO_2 thin films. *International Journal of Hydrogen Energy*, 2014, **39(36):** 21500–21511.

[22] CHOUDHURY B, CHOUDHURY A. Tailoring luminescence properties of TiO_2 nanoparticles by Mn doping. *Journal of Luminescence*, 2013, 136: 339–346.

[23] WANG R, SAKAI N, FUJISHIMA A, *et al*. Studies of surface wettability conversion on TiO_2 single-crystal surfaces. *Journal of Physical Chemistry B*, 1999, **103(12):** 2188–2194.

[24] TAKEUCHI M, ONOZAKI Y, MATSUMURA Y, *et al*. Photoinduced hydrophilicity of TiO_2 thin film modified by ar ion beam irradiation. *Nuclear Instruments & Methods in Physics Research Section B-Beam Interactions with Materials and Atoms*, 2003, **206:** 259–263.

[25] SHARMA S D, SAINI K K, KANT C, *et al*. Photodegradation of dye pollutant under UV light by nano-catalyst doped titania thin films. *Applied Catalysis B-Environmental*, 2008, **84(1/2):** 233–240.

[26] WU N L, LEE M S, PON Z J, *et al.* Effect of calcination atmosphere on TiO_2 photocatalysis in hydrogen production from methanol/water solution. *Journal of Photochemistry and Photobiology A-Chemistry*, 2004, **163(1/2):** 277–280.

[27] DEVI L G, KUMAR S G, MURTHY B N, *et al*. Influence of Mn^{2+} and Mo^{6+} dopants on the phase transformations of TiO_2 lattice and its photo catalytic activity under solar illumination. *Catalysis Communications*, 2009, **10(6):** 794–798.

[28] LIN H Y, CHOU Y Y, CHENG C L, *et al*. Giant enhancement of band edge emission based on ZnO/TiO_2 nanocomposites. *Optics Express*, 2007, **15(21):** 13832–13837.

[29] GRUJIC-BROJCIN M, SCEPANOVIC M J, DOHCEVIC-MITROVIC Z D, *et al*. Infrared study of laser synthesized anatase TiO_2 nanopowders. *Journal of Physics D-Applied Physics*, 2005, **38(9):** 1415–1420.

[30] CHING W, MO S. Electronic and optical properties of three phases of titanium dioxide: rutile, anatase, and brookite. *Physical Review B*, 1995, **51(19):** 13023–13032.

[31] WALSH A, DA Silva J L F, WEI S. Origins of band-gap renormalization in degenerately doped semiconductors. *Physical Review B*, 2008, **78(7):** 075211.

[32] SHAO G. Electronic structures of manganese-doped rutile TiO_2 from first principles. *Journal of Physical Chemistry C*, 2008, **112(47):** 18677–18685.

[33] WANG R H, XIN J H, YANG Y, *et al*. The characteristics and photocatalytic activities of silver doped ZnO nanocrystallites. *Applied Surface Science*, 2004, **227(1-4):** 312–317.

[34] XU A W, GAO Y, LIU H Q. The preparation, characterization, and their photocatalytic activities of rare-earth-doped TiO_2 nanoparticles. *Journal of Catalysis*, 2002, **207(2):** 151–157.

[35] PLESKOV Y V. Conversion of luminous energy into electrical and chemical energy in photoelectrochemical cells with semiconductor electrodes. *Soviet Electrochemistry*, 1981, **17(1):** 1–25.

一步火焰辅助热解法制备可见光响应的嵌碳 Mn 掺杂 TiO_2 微球

孙 通, 陈 阳, 马晓清, 李 忠, 李 绘, 崔晓莉

(复旦大学 材料科学系, 上海 200433)

摘 要: 通过一步火焰辅助热解法制备不同 Mn 掺杂量的嵌碳 TiO_2 微球, 利用 X 射线衍射仪(XRD)、场发射扫描电镜(FESEM)、紫外可见漫反射谱(DRS)、X 射线能谱(XPS)、拉曼光谱对其进行表征。SEM 和 XRD 结果表明所制备的 TiO_2 为微球形貌, 且具有锐钛矿晶型, XPS 和 Raman 分析表明 Mn 掺入 TiO_2 晶格, 紫外可见漫反射谱显示引入 Mn 后可增强对可见光的吸收。Mn 掺杂嵌碳 TiO_2 微球在可见光下对亚甲基蓝(MB)具有更强的降解能力。与其他方法相比, 本方法具有简单, 便捷, 对环境友好, 无需热处理的优点, 可用于制备其他金属元素掺杂的样品, 具有较大的应用潜力。

关 键 词: TiO_2; 光催化剂; 火焰辅助法; 微球; Mn 掺杂

中图分类号: TB321 **文献标识码:** A

勘 误

《无机材料学报》第 8 期中文目录:

GaSe 晶体的掺 S 生长及性能研究(英文)……杨丰柏, 陆梦晨, 张 欣, 等 (887)

应为:

GaSe 晶体的掺 S 生长及性能研究(英文)……黄昌保, 倪友保, 吴海信, 等 (887)